# Highly Stable DNA Triplexes Formed with Cationic Phosphoramidate Pyrimidine α-Oligonucleotides

Thibaut Michel,[a] Françoise Debart,*[a] Frédéric Heitz,[b] and Jean-Jacques Vasseur[a]

*The ability of cationic phosphoramidate pyrimidine α-oligonucleotides (ONs) to form triplexes with DNA duplexes was investigated by UV melting experiments, circular dichroism spectroscopy and gel mobility shift experiments. Replacement of the phosphodiester linkages in α-ONs with positively charged phosphoramidate linkages results in more efficient triplex formation, the triplex stability increasing with the number of positive charges. At a neutral pH and in the absence of magnesium ions, it was found that a fully cationic phosphoramidate α-TFO (triplex-forming oligonucleotide) forms a highly stable triplex that melts at a higher temperature than the duplex target. No hysteresis between the annealing and melting curves was noticed; this indicates fast association. Moreover, the recognition of a DNA duplex with a cationic α-TFO through Hoogsteen base pairing is highly sequence-specific. To the best of our knowledge, this is the first report of stable triplexes in the pyrimidine motif formed by cationic α-oligonucleotides and duplex targets.*

## Introduction

The ability of TFOs (triplex-forming oligonucleotides) to interact specifically with polypurine/polypyrimidine double-stranded DNA to form triplexes makes them candidates for repression of genomic transcription in the so-called antigene strategy.[1–7] Moreover, several studies have shown the promise of DNA triplexes for inducing gene recombination and repairing genetic defects in mammalian cells.[8–10]

However, several restrictions limit the use of TFOs for potential gene therapy. Of these, the most significant problem is weak binding of the third strand to the underlying DNA duplex. The hybridisation of the TFO to double-stranded DNA occurs in the major groove of the duplex and is the result of Hoogsteen or reverse-Hoogsteen hydrogen bonds between the nucleobases of the TFO and those of the duplex purine strand. In the pyrimidine-motif triplex, cytosine protonation—which occurs at a relatively acidic pH, far from physiological conditions—is required to form $C^+$·G:C triplets and consequently to ensure triplex stability. Moreover, the low stability of triplexes under physiological conditions is partly due to unfavourable charge repulsion between the three negatively charged DNA strands. As a consequence, high, nonphysiological levels of multivalent cations, such as $Mg^{2+}$,[11] or polyamines are crucial for triplex stabilisation.[12,13]

To reduce charge repulsion, the grafting of cationic amino groups to synthetic TFOs has been achieved.[14] However, up to now, very few cationic modifications have efficiently improved the ability of pyrimidine TFOs to form stable triplexes. As examples, the covalent attachment of spermine to C4 of 5-methylcytosine[15–17] or substitution of uracil-H5 with an aminopropargyl side chain[18] have produced base-modified analogues with attractive binding to duplex DNA. With regard to sugar modifications, the combination of a positive charge and an RNA-like conformation in 2′-aminoethoxy oligonucleotides (ONs) has resulted in significant increases in triplex stability even in comparison with 2′-*O*-methyl TFOs, clearly showing the cationic effect of the substitution.[19,20] Moreover, it has recently been shown that the bis-amino compound 2′-aminoethoxy-5-propargylamino-uridine dramatically enhances triplex stability.[21,22] The insertion of cationic groups into nucleobases or sugars leads to zwitterionic ONs still bearing phosphate linkages, whereas cationic backbone modifications can produce both zwitterionic and fully modified cationic ONs.[23–31] Replacement of anionic phosphodiester bonds with cationic phosphoramidates may result in favourable electrostatic interactions between the positively charged TFO and the negatively charged DNA target. In addition, cationic ONs would be expected to have better cellular permeation properties than anionic ONs.[32] Finally, cationic phosphoramidate TFOs present other advantages: they are not degraded by nucleases and their synthesis can be performed by small changes to existing automated DNA synthetic processes.

In most cases, modifications of phosphate groups induce destabilisation of the hybrids. This presumably results from the diastereoisomerism due to phosphorus chirality, in comparison with unmodified phosphodiester (PO) β-ONs. Indeed, of the mixtures of diastereoisomers, only a few possess the optimal

[a] *Dr. T. Michel, Dr. F. Debart, Dr.' J.-J. Vasseur*
*LCOBS, UMR 5625 CNRS-UMII, CC 008, Université Montpellier II*
*Place Eugène Bataillon, 34095 Montpellier Cedex 05 (France)*
*Fax: (+33) 4-6704-2029*
*E-mail: debart@univ-montp2.fr*

[b] *Dr. F. Heitz*
*CRBM, FRE 2593 CNRS*
*1919 Route de Mende, 34293 Montpellier Cedex 05 (France)*

  DOI: 10.1002/cbic.200400436 

combination of physical, chemical and biological properties.[26,33] Despite this weak binding, the replacement of PO linkages with positively charged phosphoramidate linkages in a purine TFO resulted in efficient triplex formation.[27] Moreover, these purine cationic TFOs specifically inhibited the expression of a plasmid DNA injected into *Xenopus oocytes*.[28,34]

For some years our group has been developing phosphoramidate α-anomeric ONs, which form stable parallel-stranded duplexes with complementary natural DNA and RNA.[35,36] Furthermore, we demonstrated that nonionic phosphoramidate α-ONs form more stable triplexes than their β-analogues and natural ONs.[37,38] Although interesting, the stability of these triplexes under physiological pH conditions remained low. To improve the binding of these analogues, we introduced cationic dimethylaminopropyl phosphoramidate (PNHDMAP) linkages into ONs with α-anomeric configurations (Scheme 1). We first established that the stereoisomerism of a single cationic PNHDMAP linkage introduced into an α-ON was not detrimental to the stability of hybrids formed with DNA or RNA, regardless of the isomer considered.[35] We then incorporated three to five cationic PNHDMAP linkages into phosphodiester α-dodecamers through dinucleoside building blocks containing a PNHDMAP linkage. In comparison with natural β-POs, or even with nonionic phosphoramidate α-ONs, the thermal stabilities of triplexes formed with these chimeric PO/PNHDMAP α-TFOs were considerably enhanced.[30] More recently, we showed that cationic PNHDMAP α-ONs tightly bind to RNA with high specificity and were capable of arresting RNA translation by interfering with the hepatitis C virus internal ribosome entry site in a whole-cell assay without transfecting agents.[29] These promising data have prompted us to evaluate the hybridisation properties of cationic PNHDMAP pyrimidine α-TFOs with double-stranded DNA in depth.

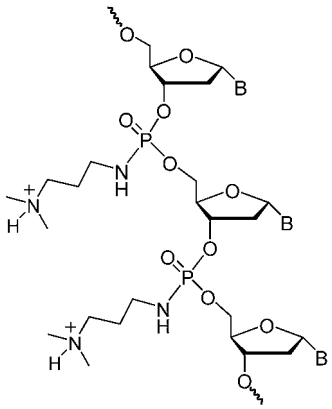

**Scheme 1.** Cationic analogues: dimethylaminopropyl-phosphoramidate (PNHDMAP) α-oligodeoxynucleotides.

In this paper we focus on the stabilities of triplexes formed with various cationic phosphoramidate pyrimidine α-TFOs containing increasing numbers of positive charges. Particularly interestingly with respect to possible therapeutic and diagnostic purposes, we show by UV melting, CD spectroscopy and gel mobility shift experiments that these cationic TFOs bind with extraordinary high affinity and specificity to their DNA targets under pH and salt conditions that approximate physiological conditions.

## Results

### Cationic α-ONs form highly stable triplexes over a wide pH range

**UV melting studies**: The thermal stabilities of complexes generated by pyrimidine α-ONs 3–5 (12 nucleotides in length) containing an increasing number (five to 11) of cationic PNHDMAP internucleotide bonds with duplex DNA targets were evaluated by UV absorption spectroscopy (Table 1). We determined melting temperatures ($T_m$s) by thermal denaturation and renaturation experiments. No differences between the thermal association and dissociation curves of the TFOs hybridised to DNA targets were observed except in the case of the unmodified PO β-TFO 1. The melting curve of duplex target I, which is preorganised in a hairpin structure (34 nucleotides in length) and contains a 12 bp polypurine:polypyrimidine region was monophasic and pH-independent ($T_m = 74$ °C). Binding of the PO β-TFO 1 occurs in a parallel orientation with respect to the purine strand of target I, by Hoogsteen base pairing. In contrast, all the phosphoramidate α-ONs obtained as diastereoisomeric mixtures bind to the DNA duplex purine strand with an antiparallel orientation as Hoogsteen third strands.[37,38]

At pH 7, the melting of the complex β-TFO 1 with duplex I remained monophasic, with only one transition at 74 °C, whereas the melting of α-TFO 3 with duplex I was biphasic,

**Table 1.** Targets and oligonucleotides synthesised.

| ON | Sequence 5′→3′[a] | Anomeric configuration of sugar[b] | Internucleotide backbone[c] |
|---|---|---|---|
| | Hairpin duplex targets | | |
| I | GC**AAAGAAGGAGAA**CTTTTG**TTCTCCTTCTTT**GC | β | PO |
| II | GC**AAAGAA*A*GAGAA**CTTTTG**TTCTC*T*TTCTTT**GC | β | PO |
| III | GC**AAAGA*GA*GAGAA**CTTTTG**TTCTC*TC*TCTTT**GC | β | PO |
| | Short-strand duplex target | | |
| IV | **AAAGAAGGAGAA** | β | PO |
| | **TTCTCCTTCTTT** | β | PO |
| | Long-strand duplex target | | |
| V | GAGG**AAAGAAGGAGAA**GAGA | β | PO |
| | TCTC**TTCTCCTTCTTT**CCTC | β | PO |
| | Pyrimidine TFO | | |
| 1 | TTTCTTCCTCTT | β | PO |
| 2 | T+T+T+C+T+T+C+C+T+C+T+T | β | 11 PNHDMAP |
| 3 | TTCT+C+C+T+T+CTTT | α | 5 PNHDMAP |
| 4 | TT+C+T+C+C+T+T+C+T+TT | α | 9 PNHDMAP |
| 5 | T+T+C+T+C+C+T+T+C+T+T+T | α | 11 PNHDMAP |

[a] Bold uppercase: TFO binding site (12-mers) in the duplex target sequences; bold, italic and underlined uppercase: mismatches in target sequences II and III; symbols +: dimethylaminopropyl-phosphoramidate backbones. [b] β-TFOs 1 and 2 have parallel orientations with respect to the purine strand of the duplex and α-TFOs 3, 4 and 5 have antiparallel orientations. [c] PO: phosphodiester; PNHDMAP: dimethylaminopropylphosphoramidate.

  

with a first transition—the melting of the triplex to a duplex—at low temperature (26.5 °C) and the second transition—the melting of the target I—at higher temperature (74 °C; Table 2).

**Table 2.** Melting temperatures ($T_m$s) of the triplexes.[a]

| Duplex target | pH | β-TFO 1 | α-TFO 3 | 4 | 5 |
|---|---|---|---|---|---|
| I[b] | 5.5 | 29.0 | 56.0 | >86.0 | n.d.[c] |
| | 6.2 | 19.0 | 44.0 | 80.0 | 85.5 |
| | 7.0 | <5 | 26.5 | 74.0 | 79.0 |
| | 7.4 | n.d.[c] | n.d.[c] | 46.0 | 74.0 |
| IV[b] | 7.0 | 7.5 | 20.5 | 42.0 | 47.5 |

[a] $T_m$ values for triplex melting are given in °C and were measured at 260 nm in NaCl (100 mM), sodium cacodylate (10 mM) buffer, $c = 3$ μM. [b] $T_m$ of the hairpin I = 74 °C and of duplex IV = 34.5 °C. [c] n.d. = no $T_m$ determined.

Interestingly, the complexes with α-TFOs 4 and 5 each showed only one transition, with $T_m$ values of 74 °C and 79 °C, respectively, which could be identified as direct melting of the triplex to its constituent single-strand DNA. The double modification—α-anomeric configuration and PNHDMAP linkages—greatly increased the thermal stability of the complexes: see, for example, the unmodified phosphodiester β-ON 1 and the fully cationic α-ON 5. In comparison, a fully nonionic methoxyethylphosphoramidate (PNHME) α-TFO formed a less stable triplex ($T_m$ = 23, 39.5 and 55 °C at pH 7, 6.2 and 5.5, respectively).[37] This stabilisation was enhanced with increasing numbers of cationic linkages in the α-TFO.

At pH 6.2, transitions due to the dissociation of TFOs 1 or 3 from the duplex I were observed, with $T_m$ values of 19 °C and 44 °C, respectively. The α-TFOs 4 and 5 each formed a complex with one transition and a $T_m$ value (80 °C and 85 °C) higher than the $T_m$ of the duplex I (74 °C). At acidic pH (5.5), the two transitions were not well resolved with α-TFO 3, and only the first parts of the melting curves were detectable below 85 °C for 4 and 5, but no $T_m$s could be determined. It is noteworthy that the $T_m$ of the complex formed with the fully cationic α-TFO 5 was extremely high even at pH 7.4 (74 °C).

As would be expected with the CT pyrimidine triplex motif, the melting profiles were pH-dependent and the $T_m$ values shifted to lower temperatures at high pH values. When the pH was increased from 6.2 to 7.0, this effect was significantly more pronounced for triplexes formed with α-TFO 3 ($\Delta T_m$ = 17.5 °C) than with α-TFOs 4 and 5 ($\Delta T_m$ = 6–6.5 °C). Similarly, when the pH was raised from 7 to 7.4, the $T_m$ of the triplex formed with α-TFO 4 dropped by 28 °C relative to pH 7 whereas with α-TFO 5 the decrease was only 5 °C. The higher the number of cationic linkages, the lower the pH dependence of the complex stability. Thus, cationic internucleotide linkages counterbalanced the destabilising effect of pH.

As these monophasic melting profiles were exceptional, we repeated UV melting experiments at pH 7 with a short duplex target IV (12 bp in length) in order to form a triplex with three separated single strands. This shorter duplex IV melts at a much lower temperature ($T_m$ = 34.5 °C) than the hairpin duplex I ($T_m$ = 74 °C; Figure 1; Table 2). The triplex with the unmodified β-TFO 1 showed two-step melting, with $T_m$ values at 7.5 °C and 34.5 °C. With α-TFO 3, the two melting transitions were not properly resolved but the low-temperature transition at 20.5 °C could be assigned to the melting of the triplex into the duplex I and the free single strand 3. On the other hand, when the number of cationic linkages was increased from five to nine or 11 in α-TFOs 4 and 5, only one transition was observed, at a higher temperature (42 °C and 47.5 °C) than for the duplex $T_m$ (34.5 °C). The stabilities of the complexes formed between 4 or 5 and their target IV were higher than that of duplex IV and in the case of the fully PNHDMAP-modified α-TFO 5 the $T_m$ was over 40 °C higher than that of the reference triplex at neutral pH.

The sharpness of the melting curve observed at 260 nm with an α-TFO was indicative of cooperativity, whereas a very broad transition ($T_m$ = 32.5 °C) was obtained with β-TFO 2, containing 11 PNHDMAP linkages (data not shown). Furthermore, it is notable that 15 minutes incubation of the samples before the melting experiments were sufficient to provide optimal binding. No differences between the hybridisation curves and the melting curves were observed with α-TFOs 3, 4 and 5, indicating fast association, whereas hysteresis was noted with the unmodified PO β-TFO 1 under the same experimental conditions. Another finding is that triplexes with the short duplex IV and the cationic α-TFO were less stable than with the longer hairpin target I. This contrasts with the already reported behav-

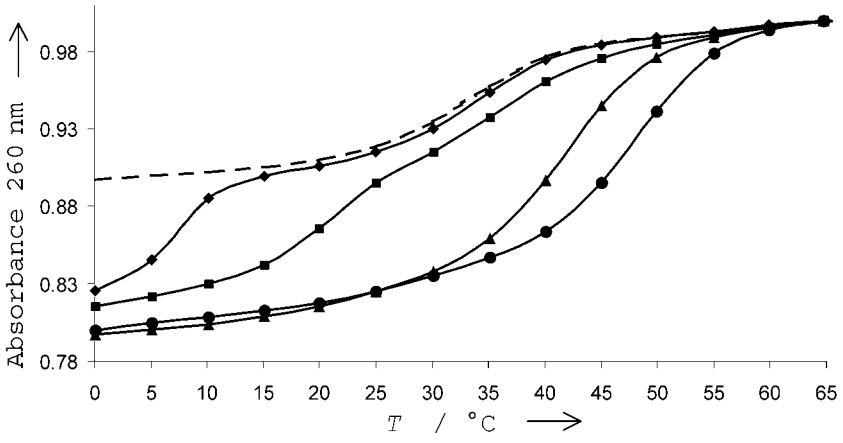


**Figure 1.** UV melting curves (260 nm) of duplex DNA IV (-----) and of the complexes formed with target IV and β-TFO 1 (◆), α-TFO 3 (■), α-TFO 4 (▲) or α-TFO 5 (●) in sodium cacodylate (10 mM), NaCl (100 mM), 3 μM, pH 7. Curves represented by using offsets, started at absorbance of 1.

  

iour of triplexes formed with β-TFOs and targets of various lengths.[39]

### Stoichiometry of complexes

To verify that the three strands (α-TFO 5, GA and CT strands of target IV) would combine to form a triplex containing one strand of each oligonucleotide,[40,41] the binding stoichiometry of the fully cationic α-TFO 5 with the duplex IV was determined by the continuous variation method (Job plot).[42] Thus, mixing curves of the absorbance vs. mole fraction of TFO 5 and target IV were constructed (Figure 2). A rising mole fraction of TFO 5 relative to target IV reduced the absorbance at 260 nm and 280 nm to an inflection point at 0.5 mole fraction. This value establishes the combination of the α-TFO 5 and the two strands of the DNA target IV in the formation of an α-TFO/DNA:DNA triplex.

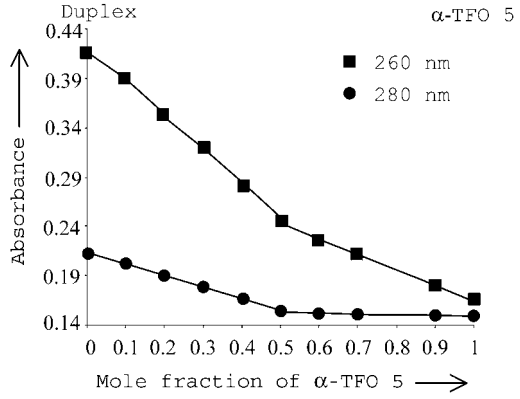


**Figure 2.** UV absorbance (260 nm and 280 nm) of mixtures of α-TFO 5 and the complementary duplex target IV at 2 μM total concentration in sodium cacodylate (10 mM), NaCl (100 mM), pH 7 and at 15 °C.

### The recognition of duplex DNA with cationic α-TFOs is sequence-specific

If the electrostatic interaction between a cationic α-TFO and an anionic double-stranded DNA in a triplex is significant, the binding could become unspecific and independent of Hoogsteen base-pairing recognition. To study the sequence specificity of the binding, α-TFOs 3, 4 and 5 were allowed to form triplexes at pH 7 with DNA hairpins II and III. These targets contain an A:T base pair—to create a Hoogsteen mismatch (C/A:T instead of C/G:C)—and two contiguous G:C and A:T base pairs to generate two Hoogsteen mismatches (T/G:C and C/A:T instead of T/A:T and C/G:C), respectively. Introduction of one C/A:T mismatch in the hybrids between cationic α-TFOs 3 or 4 and DNA target II decreased the $T_m$s by 18.5 °C ($T_m$ = 8 °C) and 14 °C ($T_m$ = 50 °C), respectively (Table 3). Two contiguous mismatches were detrimental to triplex formation by α-TFOs 3 or 4 and hairpin III ($T_m$ < 3 °C and 34 °C). Furthermore, when the pH was decreased from 7 to 6.2, the specificity was not affected, since one or two mismatches in the triplex formed by ON 3 and target II induced 20 °C or 38 °C destabilisations, respectively (Table 3). It is noteworthy that the triplex transitions

**Table 3.** Influence of one or two mismatches on the $T_m$s of triplexes.[a]

| | | | Duplex DNA target | |
|---|---|---|---|---|
| α-TFO | pH | I | II (1 mismatch) | III (2 mismatches) |
| 5 | 7.0 | 79.0 | No triplex | No triplex |
| 4 | 7.0 | 74.0 | 50.0 (−24.0)[b] | 34.0 (−40.0)[b] |
| 3 | 7.0 | 26.5 | 8.0 (−18.5)[b] | < 3.0 |
| 3 | 6.2 | 44.0 | 24.0 (−20.0)[b] | 6.0 (−38.0)[b] |

[a] $T_m$ values for triplex melting are given in °C and were measured at 260 nm in NaCl (100 mM), sodium cacodylate (10 mM) buffer, c = 3 μM. [b] $\Delta T_m$ compared to regular triplex with I.

were very broad in the case of α-TFO 4, indicating a loss of cooperativity, the $T_m$ values being determined approximately. Finally, no triplex formation was observed when the fully modified α-TFO 5 was in the presence of hairpin II or III at pH 7, only the duplex transition being detected.

### Circular dichroism

To confirm triplex formation and to gain more information on the structures of the triplexes involving β-TFOs 1/2 or α-TFOs 3–5, CD wavelength-dependent spectra were measured at different temperatures from 2 °C to 65 °C and at neutral pH. The CD spectra of the unstructured oligonucleotides are typically characterised by low-ellipticity bands in the 210–300 nm region,[43] and the formation of secondary structure is usually accompanied by large increases in ellipticity values. CD may be used to assess the interactions between duplex and third strand by comparing the CD spectrum of a mixture of the target duplex and the third strand under triplex-forming conditions to the mathematical sum of the CD spectra of the duplex and the third strand recorded separately under identical conditions.

At low temperature, the CD spectra of β-TFOs 1 and 2 each showed a positive band centred at 275 nm, followed by a wide negative band with two shoulders at 242 and 215 nm (Figure 3 A). We noted a difference only in the intensity of the positive band, which was higher for PO β-TFO 1 between 300 and 260 nm. Furthermore, when the temperature was increased to 65 °C, only minor changes in the CD spectrum of PNHDMAP β-TFO 2 were detected (Figure 3 B). The intensity of the positive band was reduced by about 14%, whereas for PO β-TFO 1 the decrease was about 30%. No change was observed in the negative bands in the 210–260 nm wavelength range.

At 2 °C, the CD spectra of α-TFOs 3, 4 and 5 were different from those of β-ONs 1 and 2, with a large negative band centred at 270 nm and a smaller one at 224 nm (Figure 3 A). Upon increasing the temperature, we observed decreases in the CD signals for the three α-TFOs (Figure 3 B). This decline (30%) was greater with ON 3, containing five PNHDMAP linkages, than with the fully backbone-modified TFO 5 (19%). As we observed for β-TFO 1 and 2, the CD spectra of α-ONs with high contents of PO linkages were more temperature-dependent.

The CD spectra of the duplex target IV (12 bp length) each exhibited a positive band in the 300–230 nm wavelength

  

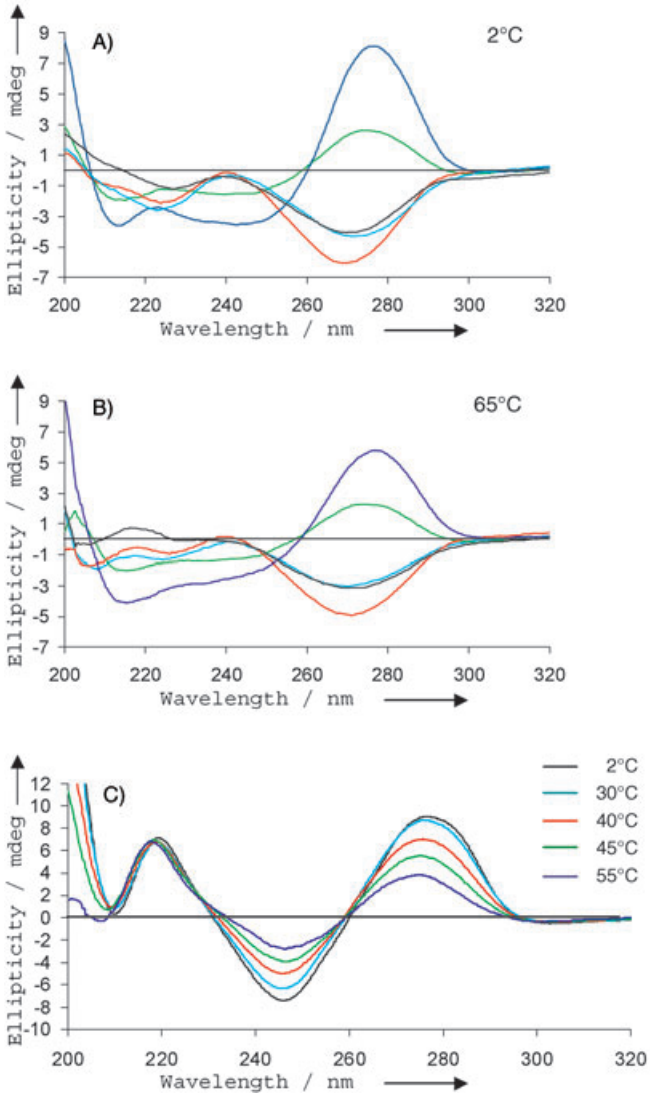


**Figure 3.** Wavelength-dependent CD spectra of single strands (30 μM): β-TFO 1 (blue), β-TFO 2 (green), α-TFO 3 (turquoise), α-TFO 4 (black), α-TFO 5 (red) at A) 2 °C and B) 65 °C, and C) of duplex IV from 2 °C to 55 °C in sodium cacodylate (10 mM), NaCl (100 mM), pH 7.

range (centred at 277 nm), a negative band of nearly equal rotational strength, centred at 245 nm and a zero crossover point at 260 nm (Figure 3C). Qualitatively, the spectra of duplex IV are characteristic of the DNA-B form.[43] From 25 °C to 65 °C, the ellipticity of the CD band located at 277 nm dramatically decreased whereas the ellipticity of the negative band located at 245 nm increased, which reflects dissociation of the duplex structure into single strands. The CD spectrum at 65 °C clearly has the shape of the denatured DNA spectrum. Below 230 nm, the spectra of duplex IV had positive ellipticity.

The CD spectrum of the mixture of duplex IV and β-TFO 1 showed one positive band centred at 277 nm and two negative bands at 245 nm and 210 nm (Figure 4A, left). In relation to the spectrum of the target duplex IV, the additional negative band at 210 nm disappeared upon increasing the temperature from 2 °C to 20 °C, whereas the intensity of the band at 245 nm did not change. The magnitude of this latter band decreased when the temperature was increased from 25 °C to 55 °C, which corresponds to the melting of the duplex IV. Difference spectra (in which the sum of the duplex and the single-strand spectra is subtracted from the mixture spectrum) showed the parts of the spectrum specific to the triplex (data not shown). As reported,[44] the negative band at 210 nm is indicative of the existence of a triplex structure in poly(d(AG).d(CT)) complexes. This characteristic feature was also observed with triplexes formed with N3′→P5′ phosphoramidate TFOs.[45] Careful analysis of the CD spectra revealed that triplex melting could be detected at 210–220 nm and duplex melting at wavelengths between 240 and 250 nm. In this way it is possible to distinguish triplex and duplex melting independently of each other by plotting the ellipticity as a function of the temperature at the selected wavelengths of 210 nm and 245 nm, respectively (Figure 4A right).[46,47] The CD melting curve of the mixture of duplex IV and TFO 1 obtained at 245 nm was completely superimposable on the curve of duplex IV alone; this indicated that the wavelength of 245 nm was ideal for following duplex melting. The CD melting curve recorded at 210 nm was distinct from the curve of duplex IV with a much lower transition ($T_m \approx 10$ °C), which corresponds to triplex melting. These selective CD melting curves are particularly useful in cases in which duplex and triplex melting overlap, as they allow the individual observation of each melting process.

The CD spectra of α-TFO 3 hybridised to duplex IV were different from spectra obtained for reference triplex with β-TFO 1 (Figure 4B). Below 30 °C they only presented two negative bands at 210 nm and 264 nm, whereas the ellipticity of the band at 210 nm increased (from −15 mdeg to −4 mdeg) with temperature (from 2 °C to 30 °C), while the band at 264 nm did not change. This result indicated the melting only of the triplex. Above 35 °C we no longer observed a negative band at 210 nm, but a new positive band centred at 218 nm appeared in the spectra from 35 °C to 65 °C. At the same time, the intensity of the negative band at 264 nm was reduced by about 42% at 65 °C and a blue shift of about 9 nm was observed with increasing temperature to 65 °C.

With α-TFOs 4 or 5, containing nine or 11 PNHDMAP linkages, the CD spectra recorded below 50 °C were very similar, one positive band at 281 nm and two negative bands centred at 248 nm and 210 nm being observed in each case (Figure 4C, left). When the temperature was increased to 65 °C the three bands weakened dramatically, even disappearing in the case of the bands at 281 nm and at 210 nm. Only the band around 250 nm still remained, but it became wide and we observed a red shift to 258 nm. Note that at 65 °C a new positive band appeared at 218 nm in both cases. The UV melting curve of the complex of ON IV and α-TFO 5 showed only a transition at pH 7 indicating an equilibrium between the triplex form and single strands. The CD melting curves of the same complex plotted at 210 nm and 248 nm were perfectly superimposable, which confirms the simultaneous melting into three strands at high temperature (Figure 4C, right).

  

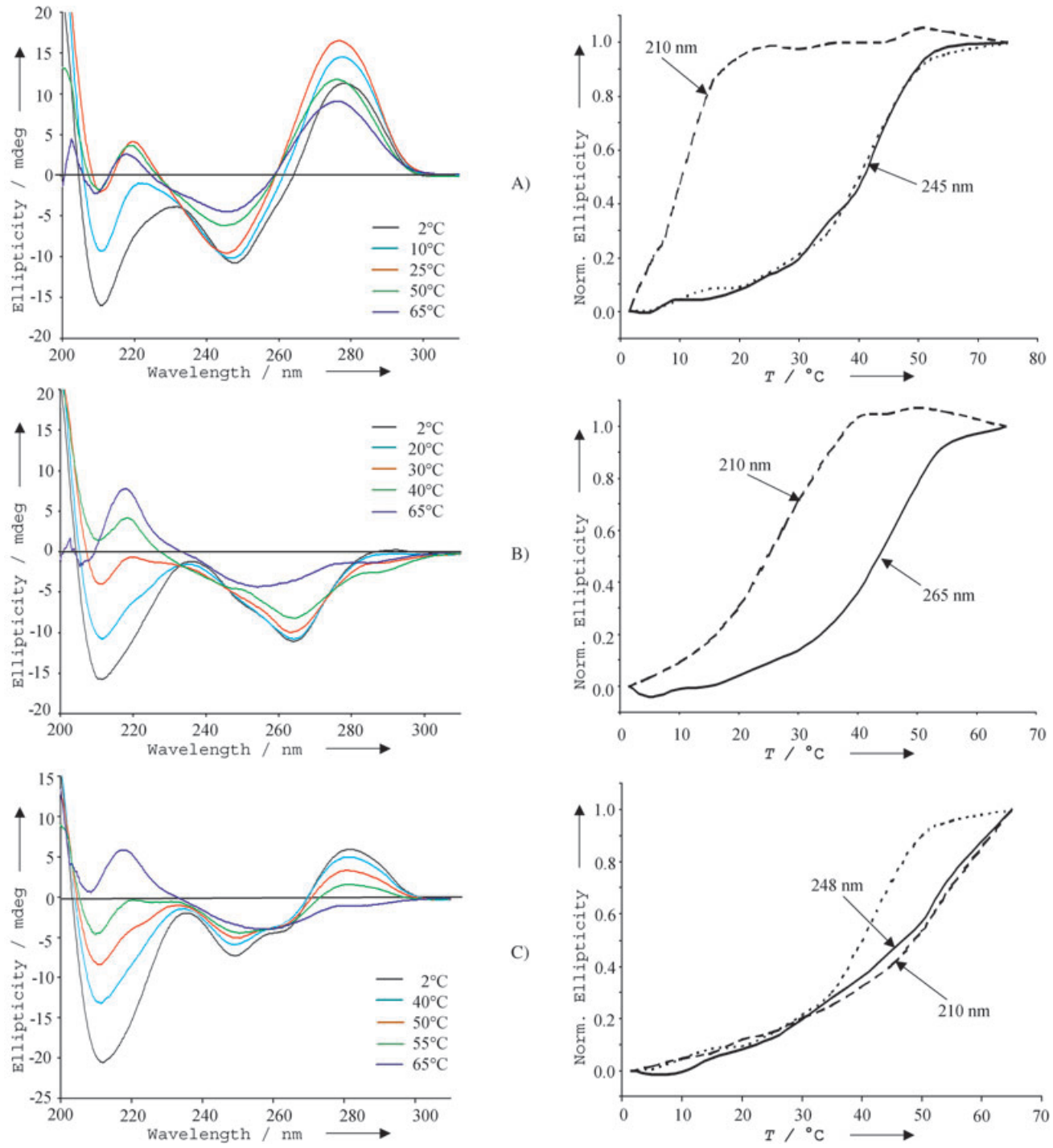


**Figure 4.** Wavelength-dependent CD spectra and CD melting curves (pH 7) for complexes with **A**) β-TFO 1 and target duplex IV: detection of triplex at 210 nm (-----) and duplex melting at 245 nm (——). **B**) α-TFO 3 and IV: detection of triplex at 210 nm (-----) and duplex melting at 265 nm (——). **C**) α-TFO 5 and IV: detection at 210 nm (-----) and 248 nm (——). CD melting curves of duplex IV in (A) and (C) are represented by dotted lines.

### Gel mobility shift assays

Formation of triplex was confirmed by EMSA (the binding of a third strand slows down the migration of the target duplex). By varying the TFO concentration (10, 100 and 1000 nM) it is possible to determine an apparent $K_D$, the concentration at which 50% of the triplex is formed. It is noteworthy that this method only gives estimations of dissociation constants ($K_D$ values are given ±30%). We performed EMSA with a 20 bp duplex V with the purine strand labelled (Figure 5). At pH 7.2 and low temperature (4°C), in the presence of NaCl (100 mM), no retarded band was observed with POs β-TFO 1 and α-TFO 3, up to 1 μM. This lack of triplex formation could be explained in terms of the pH of the medium, far from the acidic conditions necessary for the cytosine protonation required for CGC triplet stabilisation. In contrast, α-TFOs 4 and 5, contain-

  

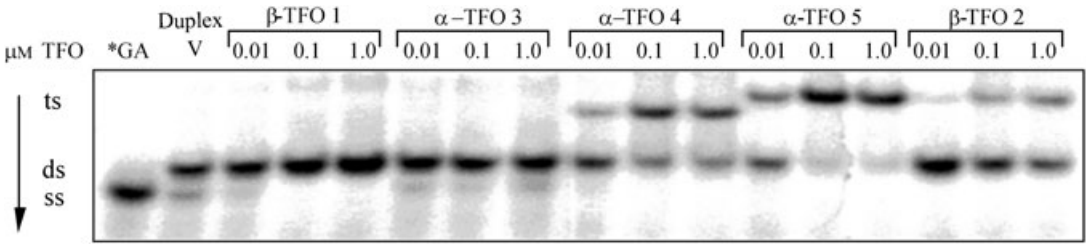


**Figure 5.** Analysis of complexes formed by α- or β-TFOs 1–5 with DNA duplex V by gel mobility shift assay at pH 7.2 and 4 °C. ss: single-stranded DNA. ds: double-stranded DNA. ts: triple-stranded DNA. The 5′-$^{32}$P-labeled purine strand is marked by an asterisk.

ing nine and 11 cationic internucleotide linkages, respectively, and β-TFO 2 showed a greater affinity for duplex V than 1 and 3. The relative intensities of the retarded bands increased with TFO concentration, except in the case of α-TFO 4, where a plateau was rapidly reached at 0.1 μM, indicating that the shift to the triplex form was incomplete. The triplex formed with α-TFO 5 was slightly more stable ($K_D = 0.02$ μM) than that formed with α-TFO 4 ($K_D = 0.06$ μM) but interestingly more stable than β-TFO 2 ($K_D > 1$ μM). The migration of the triplex formed with 5 is slightly slower than that with 4, a result of the increased cationic nature of 5. Because of the similar net charges, the mobilities of the triplex bands formed with β-TFO 2 or α-TFO 5 were similar.

## Discussion

The low strength of ON binding to a double-stranded DNA target to form a triplex is a major obstacle to their utilisation for gene targeting under physiological conditions.[10] Indeed, formation of a triple helix involves strong electrostatic repulsion between the negatively charged partner strands. Reducing the negative charge on the third strand by the introduction of cationic backbones is an attractive potential means to enhance triple helix stability. The experiments and the results described here demonstrate the potential of cationic phosphoramidate α-TFOs to overcome the limitations of unmodified TFOs.

The incorporation of cationic internucleotide linkages into a pyrimidine α-TFO increased the stability of triplexes formed with a double-stranded DNA target. The increase in $T_m$ was positively correlated to the number of cationic linkages. The α-anomeric configuration of the nucleosides compensates for the destabilisation and for the lack of melting cooperativity observed with phosphoramidate β-TFO analogues due to the mixture of diastereoisomers resulting from the phosphorus atom chirality.[26,31] In the past, we had already demonstrated that inversion of the anomeric configuration (from β to α) in fully modified nonionic *N*-alkylphosphoramidate ONs increased their affinities for single-stranded DNA and RNA[35] and for duplex DNA.[37,38] Thus, although phosphate modifications induce phosphorus chirality, the use of a diastereoisomer mixture is not detrimental for triplex formation with neutral oligonucleotides composed of α-deoxyribose units. However the α-configuration is not solely responsible for the cationic α-TFO behaviour. Indeed we recently reported that cationic α-ONs bound more tightly than nonanionic α-analogues to DNA or RNA targets.[29] Duplex DNA targeting follows the same rule. Actually, PNHDMAP α-ONs combine the stabilising effect of the α-configuration of the sugar moieties with the cationisation of the internucleotide linkages (the cationic effect) reducing the electrostatic repulsion between the strands involved in nucleic acid complexes. As a consequence, the binding strengths of cationic phosphoramidate α-TFOs to duplex DNA are higher than for their neutral analogues.

At pH 7, the triplex formed with the fully cationic α-TFO is more stable than its host duplex. The formation of a triple helix without a detectable double-helical intermediate had previously been observed for some pyrimidine TFOs producing very stable triplexes with purine targets, such as N3′→P5′ phosphoramidates,[45,48] and 2′-*O*-aminoethyl TFOs.[49] This could be explained in terms of a strong interaction between the third strand and the purine strand of the duplex. During the complex melting, the single transition can be identified as a direct melting of the triplex to its single-strand DNA constituents or by the disruption of the third-strand interaction being followed straightaway by the duplex melting.

The general observation that triplex formation is slow with unmodified pyrimidine TFOs does not hold for cationic pyrimidine α-TFOs.[50] Thus, incubation times of several hours at 4 °C are required to obtain complete triplex formation with regular TFOs, whereas cationic α-TFO binding reached its maximum within a very short incubation time. In the gel electrophoresis experiments, the samples were incubated for 17 h to allow triplex formation with PO β-TFOs, but this long incubation time was not required for triplex formation with cationic α-TFOs. Furthermore, the perfect superimposition of the melting and annealing curves shows that the triplex formation is complete during the hybridisation process of cationic α-TFOs and the rate of triplex formation is much faster than with unmodified pyrimidine TFOs under the experimental conditions used in this study.

The triplexes formed with pyrimidine cationic α-TFOs are less sensitive to pH than phosphodiester TFOs. Generally, increasing the pH lowers triplex stability due to the lack of cytosine protonation and the consequent loss of a Hoogsteen hydrogen bond in the C/G:C triplet.[51] Apparently, the cationic backbones partly compensate for the lack of cytosine protonation as the pH rises. Consequently, cationic PNHDMAP α-TFOs form stable triplexes at neutral pH. In comparison, Letsinger et al.,[26] have shown that pyrimidine ONs (15-mers) containing

  

alternating anionic PO and stereouniform cationic PNHDMAP linkages bind to duplex DNA at pH 7 to form triplexes, but only one of the zwitterionic isomers formed a relatively stable triplex ($T_m = 24\,°C$). Here, α-TFOs 3, 4 and 5 were used as diastereoisomeric mixtures and their affinities for the duplex targets were higher. Furthermore, other cationic linkages such as *N*,*N*-dimethylaminoethyl phosphoramidates incorporated into phosphodiester β-TFOs were reported to produce decreases in triplex stability with respect to the parent all-phosphate triplex.[31] In a case in which all the PO bonds were replaced by positively charged diethylaminoethyl (DEED) phosphoramidate moieties, a β-TFO was shown to associate with a duplex target with high affinity.[27] The dissociation constant for triplex formation was estimated to be 10 μM, whereas our results show a $K_D$ of 0.02 μM for the fully cationic PNHDMAP α-TFO. It seems that cationic α-TFOs bind to duplex target more efficiently than cationic β-TFOs.

In regular triplexes, high levels of $Mg^{2+}$ are generally required to neutralise the electrostatic repulsion between the negatively charged third strand and the doubly negatively charged DNA target. It is noteworthy that highly stable triplexes with the cationic α-TFOs were observed in buffers without addition of $Mg^{2+}$, due to the replacement of the electrostatic repulsion by an electrostatic attraction.

Moreover, the strong binding of a cationic PNHDMAP α-TFO to duplex DNA does not overcome the specificity due to base pairing interactions, criteria required for gene targeting. This study shows that cationic α-TFOs can discriminate between duplex DNA sequences that differ by one base pair. The specificity provides a basis for choice of TFO sequences targeted to selected sequences on duplex DNA.

Lastly, these cationic analogues are highly soluble in water, are resistant to nucleases and are taken up by the cells as previously described.[29] Taken together, all these properties indicate that cationic phosphoramidate α-TFOs have promise as sequence-specific inhibitors of gene expression, of protein binding to DNA. They should find use in a variety of applications to manipulate genes and gene function.

## Experimental Section

**Oligonucleotides synthesis and purification**: It is well established that pyrimidine-rich α-ONs and their backbone-modified phosphoramidates hybridise to the purine strand of their duplex DNA targets with an antiparallel orientation.[37,38,52] For this reason, all the PNHDMAP α-ONs described here were designed with an antiparallel orientation with respect to the DNA target purine strand.

Modified β-ON 2 and α-ONs 3–5 (Table 1) were synthesised (1 μmol scale) with an ABI model 394 DNA synthesiser by hydrogen phosphonate chemistry,[53] with protected β- or α-nucleoside 3′-*H*-phosphonates.[35,54] The elongation and the oxidation of chimeric α-ONs 3 and 4, containing mixed PO and PNHDMAP domains, were performed in blocks as previously described.[29] After deprotection with concentrated aqueous ammonia (30%) at 40 °C for 4 h, ONs 2, 4 and 5 were purified by cationic-exchange HPLC, whilst α-ON 3 was purified by anionic-exchange HPLC as reported.[29] All ONs were further desalted with Chromafix PS-RP cartridges (Macherey–Nagel). Their final purity was confirmed by HPLC and they were characterised by MALDI-TOF mass spectrometry (data not shown). Target sequences I, II, III, IV and V and unmodified ON 1 were purchased from Eurogentec (Seraing, Belgium).

**UV melting experiments**: Optical measurements were carried out on a Uvikon 943 spectrophotometer (Kontron) as previously described.[29] Prior to the experiments, the oligonucleotides, each at a final concentration of 3 μM, were mixed in NaCl (100 mM), sodium cacodylate (10 mM) buffer (pH 5.5, 6.2, 7.0, 7.4) and allowed to incubate at 90 °C for 20 min and then to cool to 5 °C. The samples were allowed to stabilise for 15 min at the beginning temperature of each heating–cooling cycle. During the melting and annealing experiments, the heating rate was fixed at $0.3\,°C\,min^{-1}$. Digitised absorbance and temperature values were stored in a computer for subsequent plotting and analysis. $T_m$ values were defined as the maximum of the first derivative plots of absorbance versus temperature.

**UV mixing curves**: Stock solutions of α-ON 5 and its complementary duplex IV were prepared at equal concentrations (of 2 μM). Job or continuous variation plots[42] were obtained by mixing samples of 5 and IV at various ratios while maintaining the total concentration at 2 μM in a 1 cm pathlength cuvette. All solutions contained sodium chloride (100 mM) and sodium cacodylate (10 mM) buffer at pH 7. Solutions were mixed and left to equilibrate at 15 °C for 20 min. After equilibration, absorbance was measured at 260 and 280 nm.

**CD measurements**: CD spectra were recorded on a JASCO J-810 spectropolarimeter interfaced with a microcomputer and equipped with a temperature controller. The cell holding chamber was flushed with a constant stream of dry nitrogen to avoid water condensation on the cell exterior. DNA samples were equilibrated for 10 min prior to each scan. For each sample, two spectrum scans were accumulated over the 200–330 nm wavelength range and the 2–65 °C temperature range in a 0.1 cm pathlength cell at a scanning rate of $20\,nm\,min^{-1}$. The oligonucleotide concentration used was 30 μM in sodium chloride (100 mM) and sodium cacodylate (10 mM) buffer (pH 7).

**Electrophoretic mobility shift assay (EMSA)**: The purine strand of duplex target V was 5′-end-labelled with [$\gamma^{32}$P ATP] (ICN 3000 $Ci\,mmol^{-1}$) and T4-polynucleotide kinase (Invitrogen) by the manufacturer's protocol. Duplex V was formed with the GA strand 5′-end-labelled and the unlabeled complementary CT strand in a 20% molar excess. Increasing concentrations of TFOs 1–5 (10 nM, 100 nM and 1 μM) were added to the target V (10 nM strand concentration). The triplex mixture in a Tris-borate-EDTA buffer (89 mM Tris, 89 mM boric acid, 2 mM EDTA, pH 7.2) containing NaCl (100 mM) was heated to 80 °C, then cooled to room temperature and incubated overnight at 4 °C and then loaded onto a 12% nondenaturating polyacrylamide gel (acrylamide/bis-acrylamide 19:1). Migration at 4 °C was carried out for 5 h (150 V) in the same buffer as described above. Gels were dried and analysed with Scion Image program. The apparent $K_d$ is defined as the TFO concentration required to shift 50% of duplex radioactivity into the retarded band (triplex).

## Acknowledgements

*We thank the Association pour la Recherche contre le Cancer for financial support (J.-J.V.).*

  

**Keywords:** anomeric configuration · cationic phosphoramidate · DNA recognition · DNA triplex · oligonucleotides

[1] K. M. Vasquez, J. M. Wilson, *Trends Biochem. Sci.* **1998**, *23*, 4 – 9.
[2] L. J. Maher, *Cancer Invest.* **1996**, *14*, 66 – 82.
[3] S. Neidle, *Anti-Cancer Drug Des.* **1997**, *12*, 433 – 442.
[4] G. Wang, D. D. Levy, M. M. Seidman, P. M. Glazer, *Mol. Cell. Biol.* **1995**, *15*, 1759 – 1768.
[5] A. Majumdar, A. Khorlin, N. B. Dyatkina, M. F. L. Lin, J. Powell, J. Liu, Z. Fei, Y. Khripine, K. A. Watanabe, J. George, P. M. Glazer, M. M. Seidman, *Nat. Genet.* **1998**, *20*, 212 – 214.
[6] K. M. Vasquez, L. Naryanan, P. M. Glazer, *Science* **2000**, *290*, 530 – 533.
[7] R. V. Guntaka, B. R. Varma, K. T. Weber, *Int. J. Biochem. Cell Biol.* **2003**, *35*, 22 – 31.
[8] B. P. Casey, P. M. Glazer, *Prog. Nucleic Acid Res. Mol. Biol.* **2001**, *67*, 163 – 192.
[9] M. P. Knauert, P. M. Glazer, *Hum. Mol. Genet.* **2001**, *10*, 2243 – 2251.
[10] M. M. Seidman, P. M. Glazer, *J. Clin. Invest.* **2003**, *112*, 487 – 494.
[11] S. W. Blume, J. Lebowitz, W. Zacharias, V. Guarcello, C. A. Mayfield, S. W. Ebbinghaus, P. Bates, D. E. Jones, Jr, J. Trent, N. Vigneswaran, D. M. Miller, *Nucleic Acids Res.* **1999**, *27*, 695 – 702.
[12] T. Thomas, T. J. Thomas, *Biochemistry* **1993**, *32*, 14068 – 14074.
[13] T. J. Thomas, G. D. Kulkarni, N. J. Greenfield, A. Shirahata, T. Thomas, *Biochem. J.* **1996**, *319*, 591 – 599.
[14] K. R. Fox, *Curr. Med. Chem.* **2000**, *7*, 17 – 37.
[15] D. A. Barawkar, V. A. Kumar, K. N. Ganesh, *Biochem. Biophys. Res. Commun.* **1994**, *205*, 1665 – 1670.
[16] D. A. Barawkar, K. J. Rajeev, V. A. Kumar, K. N. Ganesh, *Nucleic Acids Res.* **1996**, *24*, 1229 – 1237.
[17] K. J. Rajeev, V. R. Jadhav, K. N. Ganesh, *Nucleic Acids Res.* **1997**, *25*, 4187 – 4193.
[18] J. Bijapur, M. D. Keppler, S. Bergqvist, T. Brown, K. R. Fox, *Nucleic Acids Res.* **1999**, *27*, 1802 – 1809.
[19] B. Cuenoud, F. Casset, D. Hüsken, F. Natt, R. M. Wolf, K.-H. Altmann, P. Martin, H. E. Moser, *Angew. Chem.* **1998**, *110*, 1350 – 1353; *Angew. Chem. Int. Ed.* **1998**, *37*, 1288 – 1291.
[20] M. J. J. Blommers, F. Natt, W. Jahnke, B. Cuenoud, *Biochemistry* **1998**, *37*, 17714 – 17725.
[21] M. Sollogoub, R. A. J. Darby, B. Cuenoud, T. Brown, K. R. Fox, *Biochemistry* **2002**, *41*, 7224 – 7231.
[22] S. D. Osborne, V. E. C. Powers, D. A. Rusling, O. Lack, K. R. Fox, T. Brown, *Nucleic Acids Res.* **2004**, *32*, 4439 – 4447.
[23] R. L. Letsinger, C. N. Singman, G. Histand, M. Salunkhe, *J. Am. Chem. Soc.* **1988**, *110*, 4470 – 4471.
[24] P. M. Jung, G. Histand, R. L. Letsinger, *Nucleosides Nucleotides* **1994**, *13*, 1597 – 1605.
[25] T. Horn, S. Chaturvedi, T. N. Balasubramaniam, R. L. Letsinger, *Tetrahedron Lett.* **1996**, *37*, 743 – 746.
[26] S. Chaturvedi, T. Horn, R. L. Letsinger, *Nucleic Acids Res.* **1996**, *24*, 2318 – 2323.
[27] J. M. Dagle, D. L. Weeks, *Nucleic Acids Res.* **1996**, *24*, 2143 – 2149.
[28] C. P. Bailey, J. M. Dagle, D. L. Weeks, *Nucleic Acids Res.* **1998**, *26*, 4860 – 4867.
[29] T. Michel, C. Martinand-Mari, F. Debart, B. Lebleu, I. Robbins, J.-J. Vasseur, *Nucleic Acids Res.* **2003**, *31*, 5282 – 5290.
[30] F. Ehrenmann, J.-J. Vasseur, F. Debart, *Nucleosides Nucleotides Nucleic Acids* **2001**, *20*, 797 – 799.
[31] J. Robles, V. Ibanez, A. Grandas, E. Pedroso, *Tetrahedron Lett.* **1999**, *40*, 7131 – 7134.
[32] S. T. Crooke, *Methods Enzymol.* **2000**, 313, 3 – 45.
[33] A. V. Lebedev, E. Wickstrom, *Perspect. Drug Discovery Des.* **1996**, *4*, 17 – 40.
[34] J. M. Dagle, J. L. Littig, L. B. Sutherland, D. L. Weeks, *Nucleic Acids Res.* **2000**, *28*, 2153 – 2157.
[35] A. Laurent, M. Naval, F. Debart, J.-J. Vasseur, B. Rayner, *Nucleic Acids Res.* **1999**, *27*, 4151 – 4159.
[36] M. Naval, T. Michel, J.-J. Vasseur, F. Debart, *Bioorg. Med. Chem. Lett.* **2002**, *12*, 1435 – 1438.
[37] B.-W. Sun, F. Geinguenaud, E. Taillandier, M. Naval, A. Laurent, F. Debart, J.-J. Vasseur, *J. Biomol. Struct. Dyn.* **2002**, *19*, 1073 – 1081.
[38] T. Michel, F. Debart, J.-J. Vasseur, F. Geinguenaud, E. Taillandier, *J. Biomol. Struct. Dyn.* **2003**, *21*, 435 – 445.
[39] K. Yoon, C. A. Hobbs, J. Koch, M. Sardaro, R. Kutny, A. L. Weis, *Proc. Natl. Acad. Sci. USA* **1992**, *89*, 3840 – 3844.
[40] G. E. Plum, Y.-W. Park, S. F. Singleton, P. B. Dervan, K. J. Breslauer, *Proc. Natl. Acad. Sci. USA* **1990**, *87*, 9436 – 9440.
[41] Y. He, P. V. Scaria, R. H. Shafer, *Biopolymers* **1997**, *41*, 431 – 441.
[42] P. Job, *Ann. Chim. (Parid Fr.)* **1928**, *9*, 113 – 203.
[43] D. M. Gray, S.-H. Hung, K. H. Johnson, *Methods Enzymol.* **1995**, *246*, 19 – 35.
[44] V. P. Antao, D. M. Gray, R. L. Ratliff, *Nucleic Acids Res.* **1988**, *16*, 719 – 738.
[45] H. Torigoe, *Biochemistry* **2001**, *40*, 1063 – 1069.
[46] U. Parsch, K. Wörner, J. W. Engels, *Nucleosides Nucleotides* **1999**, *18*, 1641 – 1643.
[47] U. Parsch, J. W. Engels, *Chem. Eur. J.* **2000**, *6*, 2409 – 2424.
[48] B. W. Zhou-Sun, J. S. Sun, S. M. Gryaznov, J. Liquier, T. Garestier, C. Hélène, E. Taillandier, *Nucleic Acids Res.* **1997**, *25*, 1782 – 1787.
[49] N. Puri, A. Majumdar, B. Cuenoud, F. Natt, P. Martin, A. Boyd, P. S. Miller, M. M. Seidman, *Biochemistry* **2002**, *41*, 7716 – 7724.
[50] B. Faucon, J.-L. Mergny, C. Hélène, *Nucleic Acids Res.* **1996**, *24*, 3181 – 3188.
[51] N. T. Thuong, C. Hélène, *Angew. Chem.* **1993**, *105*, 697 – 723; *Angew. Chem. Int. Ed. Engl.* **1993**, *32*, 666 – 690.
[52] S. B. Noonberg, J. C. François, D. Praseuth, A.-L. Guieysse-Peugeot, J. Lacoste, T. Garestier, C. Hélène, *Nucleic Acids Res.* **1995**, *23*, 4042 – 4049.
[53] B. C. Froehler, in *Methods in molecular biology. Protocols for Oligonucleotides and Analogs*, *Vol.* 20 (Ed.: S. Agrawal), Humana Press, Totowa, **1993**, pp. 63 – 80.
[54] V. Ozola, C. B. Reese, Q. Song, *Tetrahedron Lett.* **1996**, *37*, 8621 – 8624.

Received: December 8, 2004
Published online on May 24, 2005

  